Supporting Information

Electrophilic and nucleophilic gas phase reactivity of the Janus cluster-based anions $[\{Mo_6Cl_8\}Cl_5\square]^-$ ($\square$= lacuna)

Antoine Denis,[a] Nina Tymínska,[b] Thomas Delhaye,[a] Yann Molard,[b] Pascal Gerbaux,[c] Julien De Winter,[c] Mohamed Himdi,[a] Xavier Castel,[a] Karine Costuas,*[b] Stéphane Cordier,*[b] David Rondeau*[a]

a. Univ Rennes, CNRS, Institut d'Electronique et des Technologies du numéRique – UMR 6164, F-35000 Rennes, France.

b. Univ Rennes, Ecole Nationale Supérieure de Chimie de Rennes, CNRS, Institut des Sciences Chimiques de Rennes – UMR 6226, F-35000 Rennes, France

c. Organic Synthesis and Mass Spectrometry Laboratory, Interdisciplinary Center for Mass Spectrometry (CISMa), University of Mons - UMONS, 23 Place du Parc, 7000 Mons, Belgium.

Contents

I. Experimental Section

Chemicals. HPLC-grade acetonitrile were purchased from SDS (Peypin, France). MS calibration solution containing sodium iodide (2 µg/µL) and cesium iodide (50 ng/µL) in 50/50 2-propanol/water was purchased from Sigma-Aldrich (Saint-Quentin Fallavier, France). Cesium bromide was purchased from Sigma-Aldrich (Saint-Quentin Fallavier, France).

Synthetic procedures. $Cs_2[\{Mo_6Cl^i_8\}Cl^a_6]$ was synthesized according to reported procedures with conform analytical data.[1,2]

Electrospray Ionization High Resolution Mass Spectrometry (ESI-HRMS)

The ESI-HRMS analysis of $Cs_2[\{Mo_6Cl^i_8\}Cl^a_6]$ in acetonitrile and of the mixture of $Cs_2[\{Mo_6Cl^i_8\}Cl^a_6]$/cesium bromide in acetonitrile were performed with a Waters Synapt-G2-*Si* HDMS mass spectrometer (Waters Corporation, Milford, MA) equipped with an electrospray (ESI) ionization source acting in negative ion mode. The mixture sample used, to evaluate the ion/ion reaction in gas phase, was prepared by mixing volume-to-volume the stock solution of $Cs_2[\{Mo_6Cl^i_8\}Cl^a_6]$ in acetonitrile at a 10 µg.mL^{-1} concentration with a cesium bromide solution in acetonitrile at a 2 µg.µL^{-1} concentration. The ESI-HRMS-MS experiments of the pure $Cs_2[\{Mo_6Cl^i_8\}Cl^a_6]$ cluster was performed from the stock solution. Nitrogen was used as nebulizer desolvation gas, the flow was fixed at a 600 L.h^{-1} at 150 °C (source temperature 100°C). The nebulizer gas flow was set at 6.5 bar. The capillary and cone voltages were set at -2.5 kV and -30 V, respectively. The solution was introduced into the ESI source via a syringe pump at a 5 µL.min^{-1} flow-rate. For MS-MS experiments, the quadrupole analyzer (Q) was operated in ion selection mode by setting the LM and HM resolution parameters to 4 and 1, respectively. Argon was used as collision gas. Trap collision voltage was fixed at 5 V. The full scan and MS-MS mass spectra at a 20000 resolution value (fwhm definition), were recorded between *m/z* 100 and *m/z* 2500. The data acquisition and treatment were performed using the

MassLynx v4.1 software.

Evaluation of total internal energy transmitted to the precursor ions during the collision process. Regarding mass spectrometry experiments, the maximum center-of-mass collision energy (E_{cm}) is 0.19 eV taking into account the collision energy used in the present study (5 eV) and the mass of the selected ions (*m/z* 1036).[3] Nevertheless, it is known that about 15 % of this kinetic energy (E_{kin}) is converted into internal energy (E_{int}).[4] Considering that an ion can undergo about one hundred collisions with the target gas (Ar) in the collision cell, the internal energy that can be transmitted to the ion during the overall activation process is in the order of 2.85 eV. This energy is of the same order than the enthalpy energies calculated by quantum chemical calculation for the different reactions.

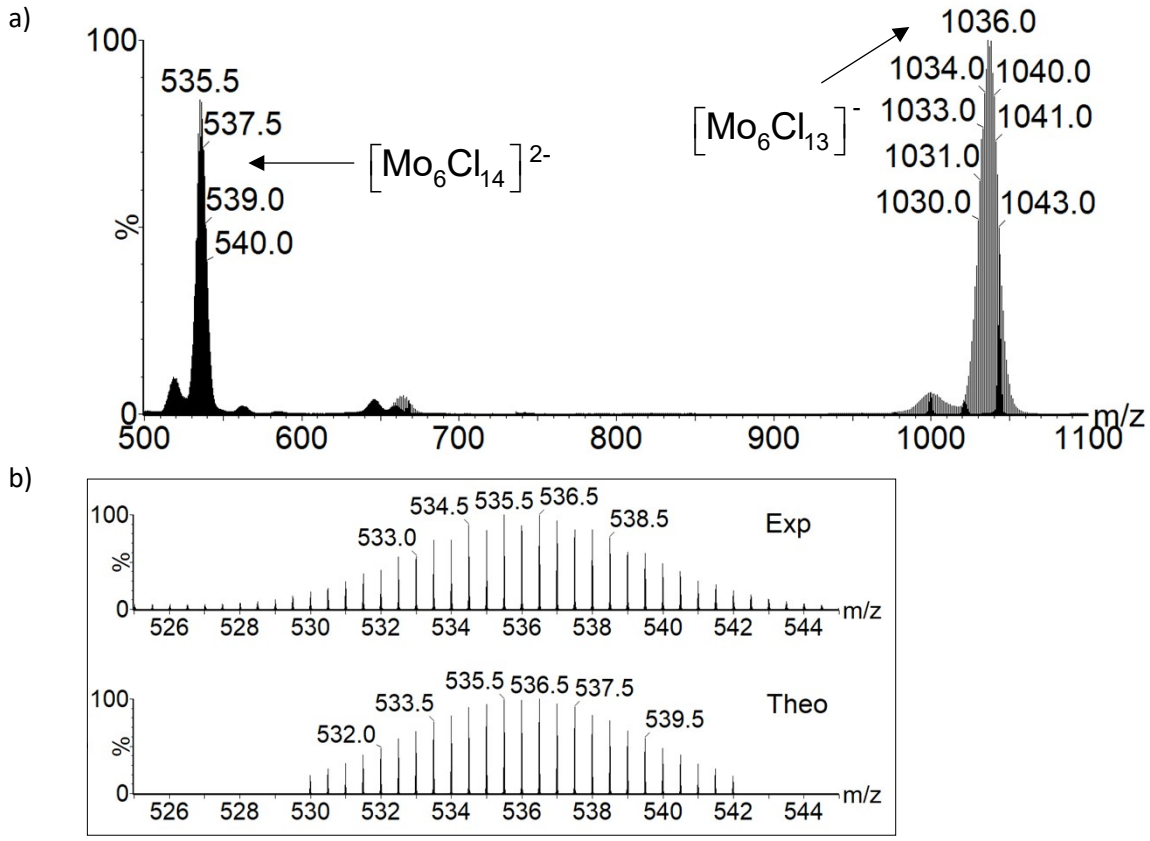

c)

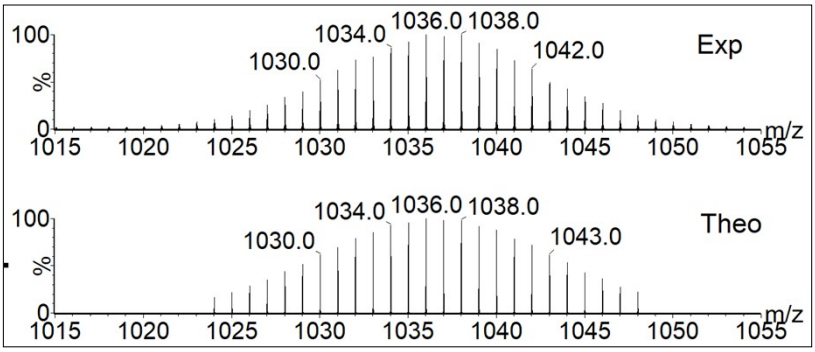

Figure S1. a) Full scan high resolution mass spectrum (R_{FWHM} = 30 000) of a $Cs_2[\{Mo_6Cl^i_8\}Cl^a_6]$ acetonitrile solution. b) Zoom in the *m/z* 525 to *m/z* 545 range of the negative ESI-high resolution spectrum showing the experimental isotopic pattern centered around *m/z* 535.5 (top) and the theoretical (bottom) isotopic distribution calculated for a 2-charged ion of Mo_6Cl_{14} elemental formulae. c) Zoom in the *m/z* 1015 to *m/z* 1055 range of the negative ESI-high resolution spectrum showing the experimental isotopic pattern centered around *m/z* 1036 (top) and the theoretical (bottom) isotopic distribution calculated for a monocharged ion of Mo_6Cl_{13} elemental formulae.

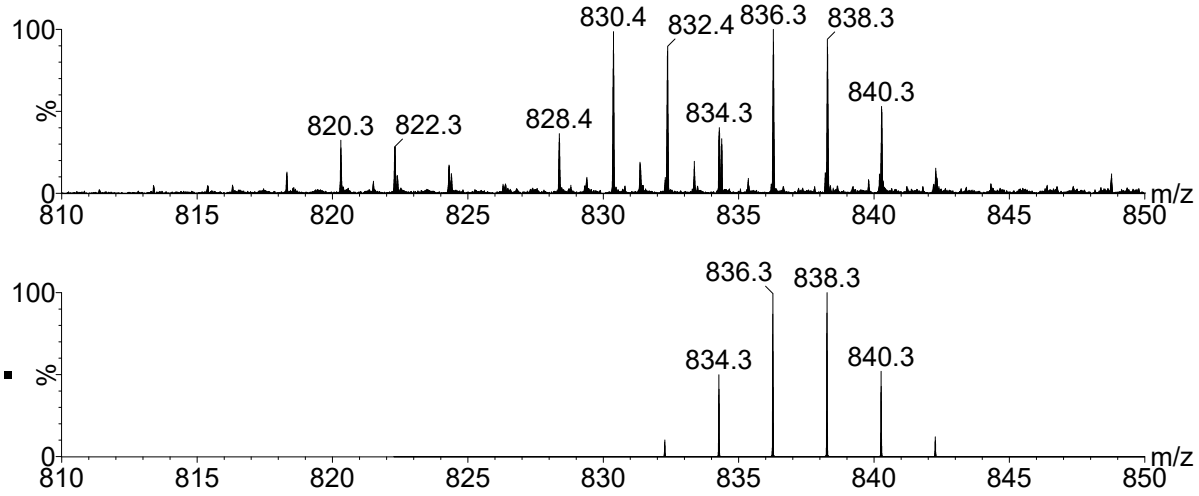

Figure S2. Top: experimental isotopic pattern in the *m/z* 810 to *m/z* 850 range of the negative ESI-MS-MS spectrum (Fig. 4 in the main text) of the $[Mo_6Cl_{13}]^-$ and $[Cs_4KBr_6]^-$ ions selected in a mass range encompassing the two isotopic patterns centered around the *m/z* 1036 value. Bottom: theoretical isotopic distribution calculated for a monocharged ion of Cs_3KBr_5 elemental formulae.

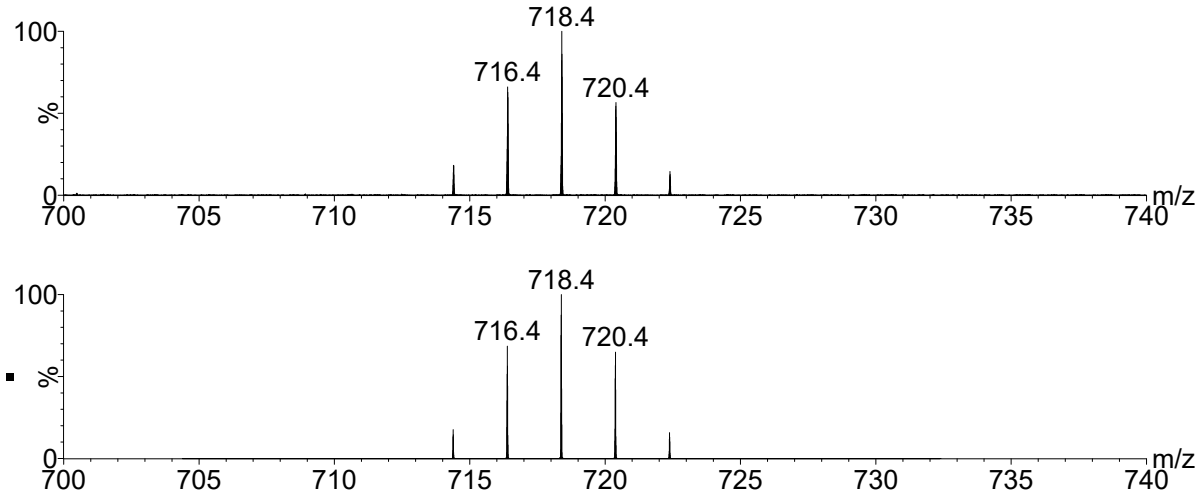

Figure S3. Top: experimental isotopic pattern in the *m/z* 700 to *m/z* 740 range of the negative ESI-MS-MS spectrum (Fig. 4 in the main text) of the $[Mo_6Cl_{13}]^-$ and $[Cs_4KBr_6]^-$ ions selected in a mass range encompassing the two isotopic patterns centered around the *m/z* 1036 value. Bottom: theoretical isotopic distribution calculated for a monocharged ion of Cs_3Br_4 elemental formulae.

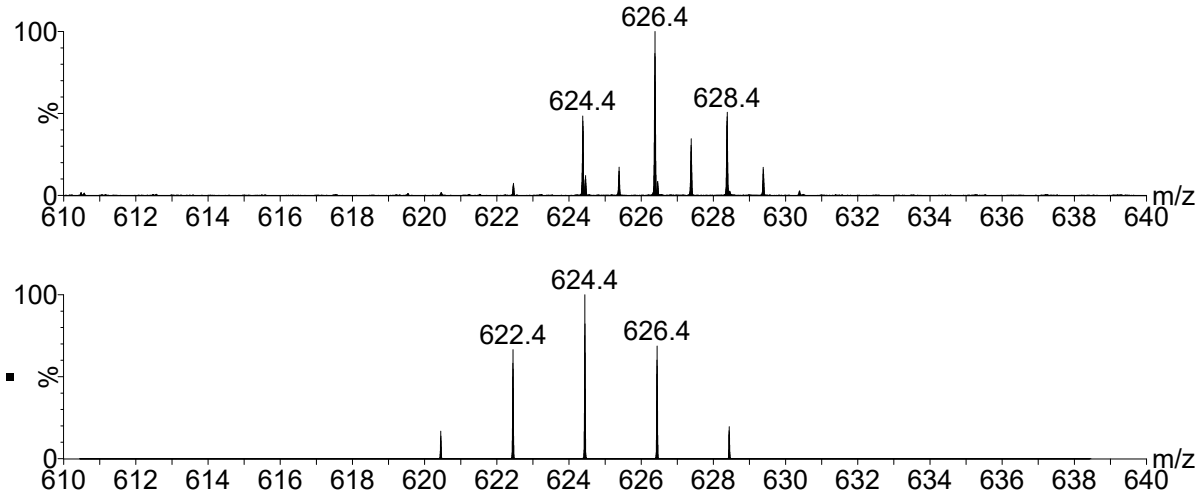

Figure S4. Top: experimental isotopic pattern in the *m/z* 610 to *m/z* 640 range of the negative ESI-MS-MS spectrum (Fig. 4 in the main text) of the $[Mo_6Cl_{13}]^-$ and $[Cs_4KBr_6]^-$ ions selected in a mass range encompassing the two isotopic patterns centered around the *m/z* 1036 value. Bottom: theoretical isotopic distribution calculated for a monocharged ion of Cs_2KBr_4 elemental formulae.

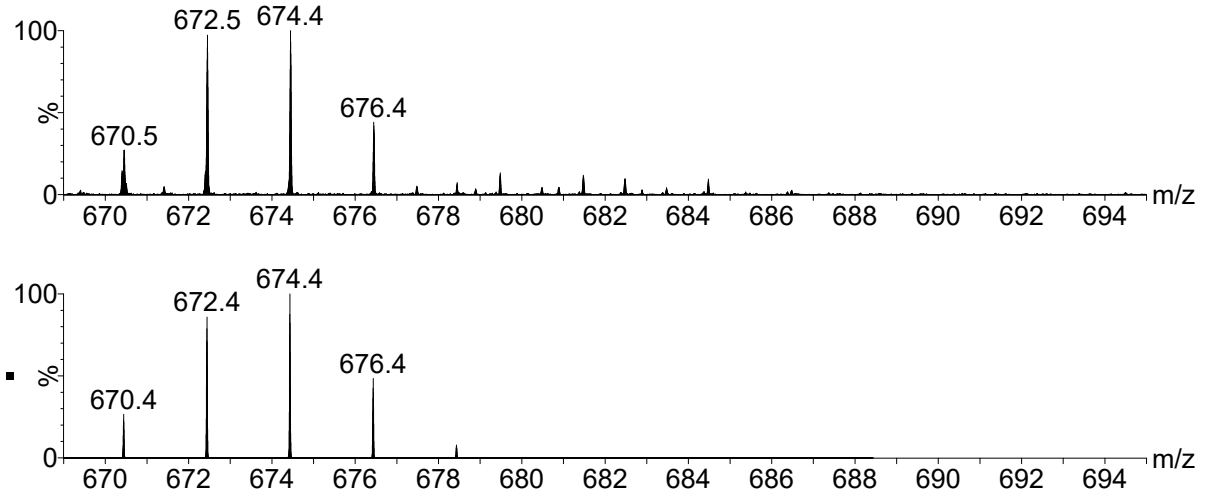

Figure S5. Top: experimental isotopic pattern in the *m/z* 669 to *m/z* 695 range of the negative ESI-MS-MS spectrum (Fig. 4 in the main text) of the $[Mo_6Cl_{13}]^-$ and $[Cs_4KBr_6]^-$ ions selected in a mass range encompassing the two isotopic patterns centered around the *m/z* 1036 value. Bottom: theoretical isotopic distribution calculated for a monocharged ion of Cs_3Br_3Cl elemental formulae.

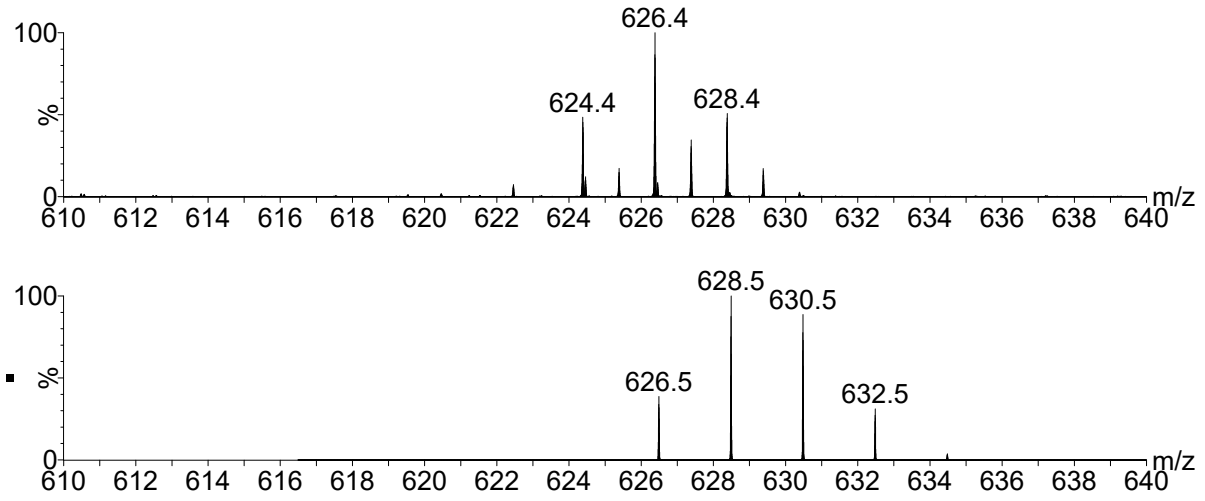

Figure S6. Top: experimental isotopic pattern in the *m/z* 610 to *m/z* 640 range of the negative ESI-MS-MS spectrum (Fig. 4 in the main text) of the $[Mo_6Cl_{13}]^-$ and $[Cs_4KBr_6]^-$ ions selected in a mass range encompassing the two isotopic patterns centered around the *m/z* 1036 value. Bottom: theoretical isotopic distribution calculated for a monocharged ion of $Cs_3Br_2Cl_2$ elemental formulae.

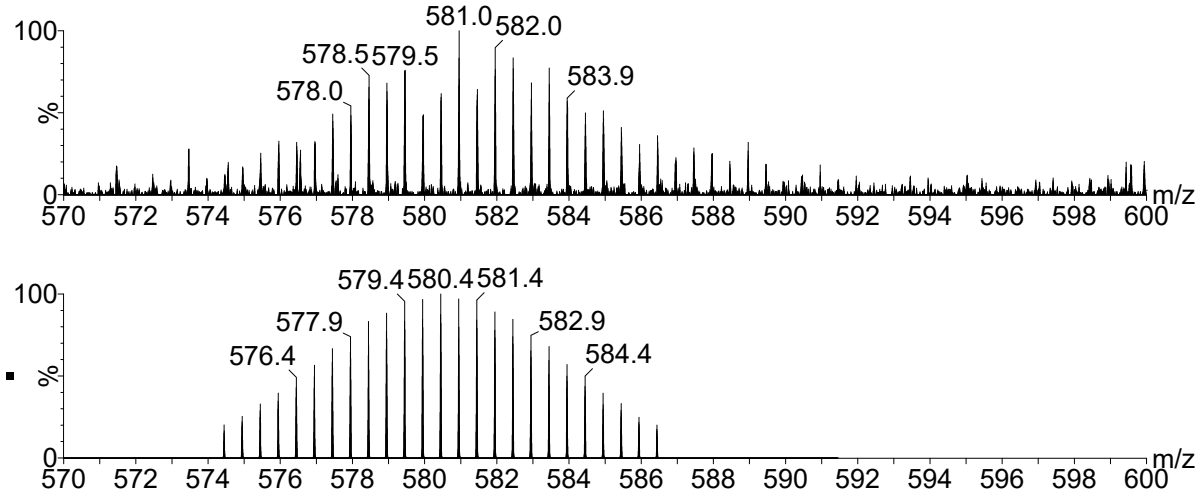

Figure S7. Top: experimental isotopic pattern in the *m/z* 570 to *m/z* 600 range of the negative ESI-MS-MS spectrum (Fig. 4 in the main text) of the $[Mo_6Cl_{13}]^-$ and $[Cs_4KBr_6]^-$ ions selected in a mass range encompassing the two isotopic patterns centered around the *m/z* 1036 value. Bottom: theoretical isotopic distribution calculated for a 2- charged ion of $Mo_6Cl_{12}Br_2$ elemental formulae.

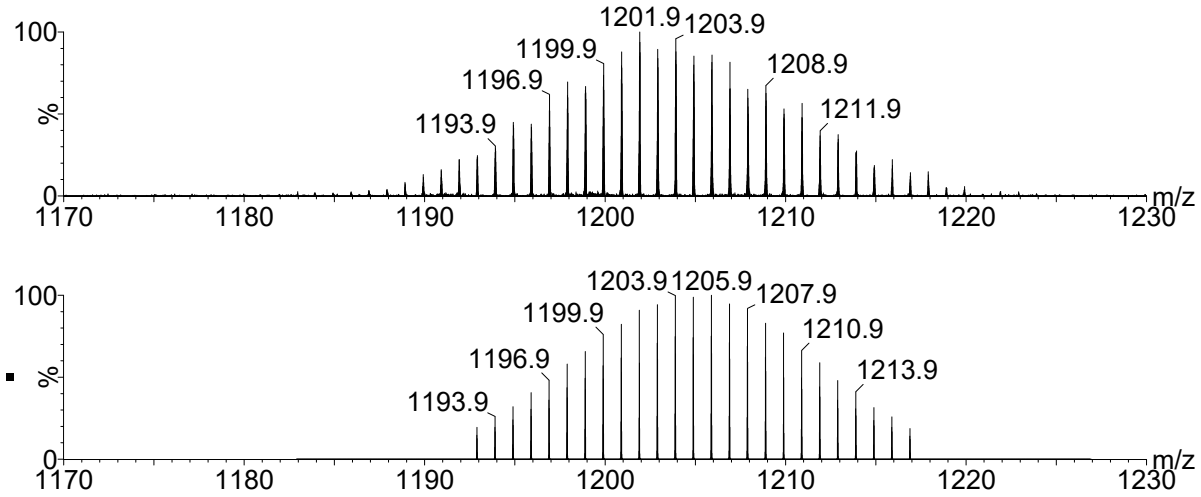

Figure S8. Top: experimental isotopic pattern in the the *m/z* 1170 to *m/z* 1230 range of the negative ESI-MS-MS spectrum (Fig. 4 in the main text) of the $[Mo_6Cl_{13}]^-$ and $[Cs_4KBr_6]^-$ ions selected in a mass range encompassing the two isotopic patterns centered around the *m/z* 1036 value. Bottom: theoretical isotopic distribution calculated for a monocharged ion of $CsMo_6Cl_{14}$ elemental formulae.

II. Computational study

Computational details. DFT calculations were carried out using ADF implemented in Amsterdam Modeling Suite (AMS 2020.101) program package developed by Baerends and co-workers.[5,6] The revPBE exchange and correlation non-local gradient corrections were added to the local density approximation description.[7,8] Relativistic spin-orbit (SO) coupling was treated at the first-order perturbation theory using a ZORA Hamiltonian.[9,10] The all electron ADF QZ4P Slater-type basis set was used, *i.e.*, a quadruple-ζ STO basis set completed with four polarization functions. Dispersion correction developed by Grimme and collaborators were included in the calculations (DFT-D3-BJ).[11] Geometry optimizations of the $[\{Mo_6Cl^i_8\}Cl^a_4\square^a_2]$ ($\square^a$ in trans and cis position), $[\{Mo_6Cl^i_8\}Cl^a_5\square^a]^-$ and $[\{Mo_6Cl^i_8\}Cl^a_6]^{2-}$ cluster units were performed. Vibrational frequency calculations were done to ensure that they are minima on the potential energy surface. For the heterolytic bond dissociation energy calculations, the basis set superposition errors were evaluated employing the counterpoise method of Boys and Bernardi.[12] Fukui functions have been calculated for $[\{Mo_6Cl^i_8\}Cl^a_5\square^a]^-$ to evaluate the electrophilic and nucleophilic attacks.[13,14,15]

Cartesian coordinates of the optimized Mo_6 clusters

trans-$[\{Mo_6Cl^i_8\}Cl^a_4\square^a_2]$

Mo	-0.001865	1.855547	-0.003579
Mo	-0.000479	-0.001259	-1.821713
Mo	1.856798	-0.001000	-0.004057
Mo	-1.858408	-0.003114	-0.004726
Mo	0.000249	-1.859659	-0.005220
Mo	-0.001131	-0.002869	1.813868
Cl	-1.746733	1.740669	1.784564
Cl	1.744659	-1.744409	-1.792183
Cl	1.744461	-1.746391	1.783654
Cl	-0.003195	4.213389	-0.003015
Cl	4.214648	0.000324	-0.004220
Cl	-4.216252	-0.004476	-0.005719
Cl	0.001610	-4.217502	-0.006815
Cl	-1.744672	-1.748437	1.783029

Cl	1.742673	1.743870	-1.790605
Cl	-1.743642	-1.746402	-1.792804
Cl	-1.745606	1.741913	-1.791227
Cl	1.742479	1.742663	1.785183

cis-[{$Mo_6Cl^i_8$}$Cl^a_4\square^a_2$]

Mo	0.004701	1.857734	-0.009833
Mo	0.007773	-0.001188	-1.873706
Mo	1.869114	-0.000965	-0.014118
Mo	-1.801135	-0.003090	-0.013193
Mo	0.006845	-1.861787	-0.011527
Mo	0.009831	-0.002854	1.796657
Cl	-1.782415	1.728267	1.777868
Cl	1.753661	-1.755004	-1.759427
Cl	1.749796	-1.746328	1.782186
Cl	0.010673	4.214625	-0.016288
Cl	0.023446	-0.000078	-4.232055
Cl	4.227143	0.000349	-0.032241
Cl	0.015373	-4.218665	-0.020129
Cl	-1.780487	-1.735982	1.776384
Cl	1.751678	1.754505	-1.757820
Cl	-1.786697	-1.746809	-1.752726
Cl	-1.788637	1.742299	-1.751077
Cl	1.747826	1.742588	1.783767

[{$Mo_6Cl^i_8$}$Cl^a_5\square^a$]$^-$

Mo	-0.001712	1.852629	-0.010969
Mo	-0.000457	-0.001234	-1.870327
Mo	1.853867	-0.000959	-0.011366
Mo	-1.855446	-0.002948	-0.012023
Mo	0.000185	-1.856675	-0.012541
Mo	-0.001154	-0.002876	1.791990
Cl	-1.752602	1.746202	1.792321
Cl	1.757261	-1.757400	-1.764990
Cl	1.750076	-1.751985	1.791557
Cl	-0.003313	4.250071	-0.012938
Cl	-0.000001	0.000074	-4.267740
Cl	4.251306	0.000104	-0.014542
Cl	-4.252896	-0.004684	-0.016048
Cl	0.001631	-4.254137	-0.016782
Cl	-1.750311	-1.753991	1.791019
Cl	1.755582	1.756988	-1.763168
Cl	-1.756209	-1.759325	-1.765716
Cl	-1.758548	1.754763	-1.763858
Cl	1.748335	1.748315	1.792796

[{$Mo_6Cl^i_8$}Cl^a_6]$^{2-}$

Mo	-0.001011	1.849442	0.000120
Mo	-0.000544	-0.001347	-1.852176
Mo	1.851236	-0.001075	-0.000864
Mo	-1.851712	-0.002845	-0.000372
Mo	0.000655	-1.853570	-0.001457

Mo	-0.000028	-0.002966	1.850829
Cl	-1.764494	1.758676	1.763206
Cl	1.762674	-1.763433	-1.765000
Cl	1.763438	-1.764696	1.761618
Cl	-0.002373	4.292021	0.000870
Cl	0.000051	0.001309	-4.294776
Cl	4.293796	0.001299	-0.002078
Cl	-4.294300	-0.005437	0.000637
Cl	0.001169	-4.296162	-0.001155
Cl	-1.761692	-1.766444	1.762425
Cl	1.761570	1.763055	-1.762654
Cl	-1.761863	-1.765424	-1.764405
Cl	-1.764368	1.760620	-1.762408
Cl	1.762817	1.761114	1.762138
Cl	0.000348	-0.001791	4.293414

References

1. K. Kirakci, S. Cordier and C. Perrin, *Z. Anorg. Allg. Chem.*, 2005, **631**, 411-416.
2. N. Saito, P. Lemoine, N. Dumait, M. Amela-Cortes, S. Paofai, T. Roisnel, V. Nassif, F. Grasset, Y. Wada, N. Ohashi and S. Cordier, *J. Clus. Sci.*, 2017, **28**, 773-798.
3. Using the well-known equation $E_{cm} = (E_{lab} \times M_{gaz}) / (M_{gaz} + M_{ion})$, where E_{lab} is the collision energy, M_{gaz} and M_{ion} are the mass of the target gas and the ion, respectively.
4. a) R. M. A. Heeren, K. Vékey, *Rapid Commun. Mass Spectrom*., 1998, **12**, 1175-1181. b) G. Chen, R. G. Cooks, D. M. Bunk, M.J . Welch, J. R. Christies, *Int. J. Mass Spectrom*., 1999, **185/186/187**, 75-90. c) L. Drahos and K. Vékey, *J. Mass Spectrom*., 2001, **36**, 237-263. d) F. Muntean and P.B. Armentrout, *J. Chem. Phys*., 2001, **115**, 1213-1228. e) J. Sztáray, A. Memboeuf, L. Drahos and K. Vékey, *Mass Spectrom. Rev.*, 2011, **30**, 298-320.
5. G. te Velde, F. M. Bickelhaupt, E. J. Baerends, C. Fonseca Guerra, S. J. A. van Gisbergen, J. G. Snijders and T. Ziegler, *J. Comp. Chem.*, 2001, **22**, 931-967.
6. AMS 2022.1*, Amsterdam, The Netherlands,* http://www.scm.com.
7. S. H. Vosko, L. Wilk and M. Nusair, *Can. J. Phys.*, 1980, **58**, 1200-1211.
8. Y. K. Zhang and W. T. Yang, *Phys. Rev. Lett.*, 1998, **80**, 890-890.
9. E. van Lenthe, A. Ehlers and E. J. Baerends, *J. Chem. Phys.*, 1999, **110**, 8943-8953.
10. E. van Lenthe and E. J. Baerends, *J. Comp. Chem.*, 2003, **24**, 1142-1156.
11. S. Grimme, S. Ehrlich and L. Goerigk, *J. Comp. Chem.*, 2011, **32**, 1456-1465.
12. S. F. Boys and F. Bernardi, *Mol. Phys.*, 1970, **19**, 553-566.
13. R. G. Parr, L. Von Szentpaly and S. B. Liu, *J. Am. Chem. Soc.*, 1999, **121**, 1922-1924.

12. C. Morell, A. Grand, A. Toro-Labbe and H. Chermette, *J. Mol. Model.*, 2013, **19**, 2893-2900.
13. G. Hoffmann, V. Tognetti and L. Joubert, *J. Mol. Model.*, 2018, **24**, 281 (1-12).